

Time-lapse well log analysis, fluid substitution, and AVO

YING ZOU and LAURENCE R. BENTLEY, University of Calgary, Alberta, Canada

Time-lapse seismic monitoring of reservoirs is based on changing seismic response due to fluid saturation, temperature, and pressure changes. The observable changes in seismic response can help locate bypassed oil, water- or gas-flood fronts, and heated zones.

However, there are risks associated with a 4D seismic project including false anomalies caused by acquisition, processing artifacts, and the ambiguity of seismic interpretation in relating seismic changes to reservoir changes. Lumley and Behrens (1998) proposed a four-step feasibility and risk assessment study before undertaking a 4D seismic project. The proposed third step is seismic modeling from sonic and density logs. Our study demonstrates a procedure for the modeling of time-lapse seismic response changes due to simulated changes to well logs. We also simulate AVO changes at a gas-oil contact (GOC) and an oil-water contact (OWC). The objective of time-lapse AVO is to distinguish between reflections from a gas or oil sand that has been flooded by gas or water. As a model, we use a well log from White Rose Field, offshore Newfoundland, Canada. Three production scenarios are investigated. The method for calculating the seismic response changes is based on the Gassmann equation and a modification of the procedure described by Bentley et al. (2000).

Theory and method. Gassmann's equation relates the bulk modulus of a saturated rock (K_u), to the dry rock bulk modulus (K_d), the solid grain modulus (K_s), the fluid bulk modulus (K_f), and the porosity ϕ . Densities are calculated from

$$\rho_f = S_g \rho_g + S_o \rho_o + S_w \rho_w \quad (1)$$

$$\rho_o = \frac{\rho_o^{std} + R_s \rho_g^{std}}{B_o} \quad (2)$$

$$\rho_u = \rho_s (1 - \phi) + \rho_f \phi \quad (3)$$

where $\rho_o, \rho_g, \rho_w, \rho_s, \rho_u, \rho_f$ are the densities of oil, gas, water, solid grains, saturated reservoir rock, and fluid mixture at reservoir conditions. $S_g, S_o,$ and S_w are gas saturation, oil saturation, and water saturation, respectively. The density ρ^{std} is the density of oil or gas at standard conditions. R_s is the gas oil ratio and B_o is the oil formation volume factor. The equations of Batzle and Wang are used to calculate $\rho_g, K_g, \rho_w,$ and K_w (adiabatic) using the known reservoir pressure, temperature, gas specific gravity, and water salinity. From equations 1 and 2, we obtain ρ_f and from 3 we get undrained rock density ρ_u . We get $\phi, \rho_s,$ and K_s from core tests.

Using empirical equations developed by Vasquez and Beggs (1980), the compressibility of the oil C_o ($K_o=1/C_o$) is calculated knowing the specific gravity of gas, separator pressure and temperature, and oil API gravity. The fluid mixture bulk modulus is calculated as a combination of the arithmetic average of fluid densities (patchy fluid saturation case) and the harmonic average (homogeneous fluid saturation case) of fluid densities (Mavko and Mukerji, 1998). The undrained bulk and shear moduli before production are computed from P- and S-velocity, and density logs using $K_u = \rho_u (V_p^2 - 4/3 V_s^2)$ and $\mu_u = \rho_u V_s^2$. K_d is calculated from K_u , the porosity, a given value of K_s and an estimate of K_f using the Gassmann equation.

New reservoir pressure, temperature, and saturations are

Table 1. Mean (M) change, mean percentage change (%), and their standard deviation (std) in oil leg zone due to fluid substitution, gas drive case

Gas drive	K_u GPa	ρ_u Kg/m ³	V_p m/s	V_s m/s	AIP Kg/sm ²
M	-0.44	-43.85	15.74	23.64	-148851
std	.14		10.13	1.13	14463.7
%	-2.3	-1.9	.4	.9	-1.5
std	.009		.002	.0001	.002

Table 2. Mean changes (M), mean percentage change (%), and their standard deviation (std) in oil leg zone due to fluid substitution, water drive case

Water drive	K_u GPa	ρ_u Kg/m ³	V_p m/s	V_s m/s	AIP Kg/sm ²
M	0.84	23.56	24.13	-12.43	157414
std	0.26		16.13	0.59	33322.5
%	4.4	1.0	0.6	-0.5	1.6
std	.017		.004	.0001	.004

specified for the postproduction conditions. Modified gas, oil, and water bulk moduli and densities are computed—again using the equations of Batzle and Wang but with the newly specified reservoir conditions. Equations 1 and 3, the new fluid density, the new fluid saturation, the porosity, and the solid grain density are used to calculate the new undrained bulk density. The percentage change in undrained bulk density is calculated using the new and old calculated undrained bulk densities. The original density logs are multiplied by the percentage change to generate an updated density log. The updated fluid bulk moduli are used with the Gassmann equation to update the undrained bulk modulus. The new bulk modulus and density values are used to update the velocity logs.

An example. White Rose Field is in Jeanne d'Arc Basin offshore Newfoundland. Husky Oil drilled the White Rose L-08 well during the spring of 1999. The geology consists of a thick section of Tertiary shales separated from Cretaceous shales by an unconformity. Gas and oil were discovered in the underlying Cretaceous Avalon sands. Figure 1 shows segments of a density log, a P-wave log and a corridor stack from a down-hole VSP survey. A wavelet was extracted from the VSP corridor stack, applied to the original logs, and zero-offset synthetic traces were generated. We used vendor software to tie synthetic traces with corridor stack and to do the AVO modeling. In the oil leg, the average porosity is 0.19, the average connate water saturation is 0.2, reservoir pressure is 29.4 MPa, reservoir temperature is 106°C, the gas oil ratio is 24.0 Sm³/Sm³, and the oil formation volume factor is 1.37 m³/Sm³. The specific gravity of gas is 0.734 and the oil API° is 31. White Rose Field has not been produced to date. In this study, we investigate three production scenarios.

- 1) Gas drive through the whole oil leg. Oil is replaced by gas. Residual oil is 0.3, and connate water is 0.22.
- 2) Water drive through the whole oil leg. Oil is replaced by

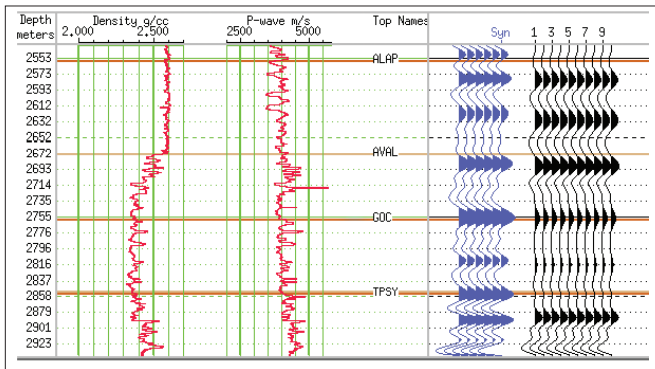


Figure 1. The original logs (red), the synthetic trace (blue), and the VSP corridor stack (black).

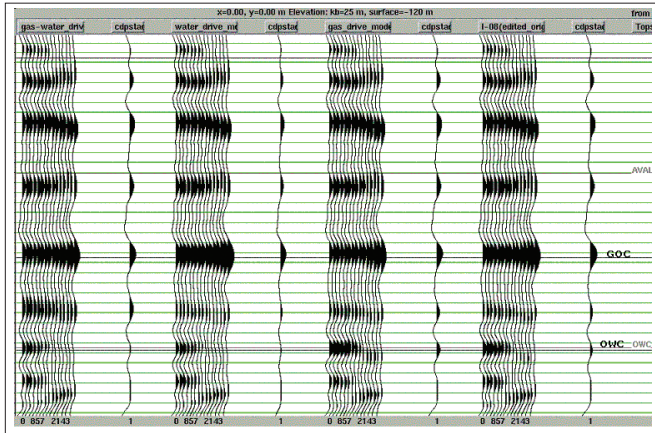


Figure 2. AVO modeling (left to right) for gas/water, water, gas drive, and original logs.

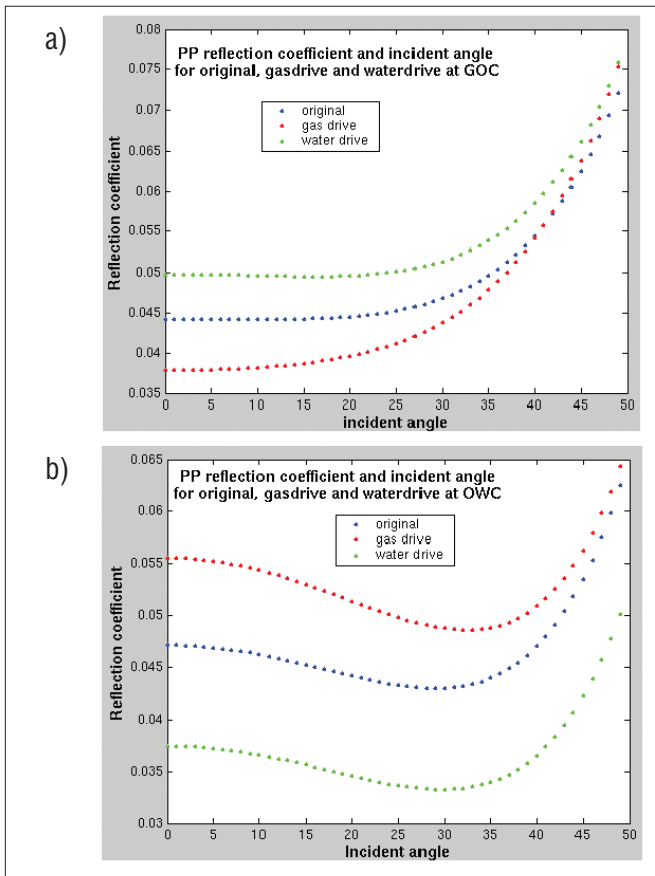


Figure 3. P-P reflection coefficient changes with incident angle for (a) at GOC and (b) at OWC.

water. Residual oil is 0.3, and there is no gas saturation. 3) Half of the oil leg is replaced by gas, and the other half is replaced by water.

All scenarios assume that reservoir pressure and temperature are maintained at initial levels.

Discussion. Tables 1 and 2 summarize the changes due to fluid substitution. For the gas drive, the bulk modulus decreases 2.3%, but the P-wave velocity increases 0.4% due to a 1.9% decrease in density. The S-wave velocity increases 0.9%. The velocity changes are small due to the large value of K_d compared to the pore fluid contribution to K_u . For the water drive case, the P-wave velocity increases 0.6%, the S-wave average velocity decreases 0.5%, and the average bulk modulus increases 4.4%. Although the percentage changes in density and velocity are small, they lead to changes in the reflection coefficients from the original GOC and OWC on the order of 15%.

Figure 2 compares the AVO effects of the three drive mechanisms with the original log case using Zoeppritz equations. The fluid substitutions cause minor changes to the AVO gradient but they do change the reflection amplitudes. The amplitude at the GOC decreased slightly in the gas drive scenario and increased in the water drive scenario compared to the original case. At the OWC the amplitude increased slightly in the gas drive scenario and decreased in the water drive scenario. The dual drive mechanism creates a new GWC. At the new GWC in the middle of oil leg, the reflection is clearer than the original case. Figure 3 shows the P-P reflection coefficient versus offset for the GOC and OWC using averaged velocity and density over a 10-m interval above and below the interface. The AVO gradients are nearly the same for all scenarios but the zero-offset values are different for each case. At the original GOC, the P-P reflection coefficient is nearly constant until offset angles of 20-25° at which point it increases with increasing angle. At the original OWC, the P-P reflection coefficient is approximately constant until about 10° where it decreases slightly until 30-35° and then increases. The main differences are in the amplitude of the reflection coefficients, which vary between 0.037 and 0.045.

Figures 4-6 show the before and after fluid substitution synthetic gathers with 20% noise added, the difference traces, the stacked gathers, and the stacked trace differences. As before, the amplitude decreases at GOC and increases at OWC for the gas drive case and the opposite for the water drive case. Again, for the gas/water drive case, the largest amplitude difference is at the new GWC, the second largest difference is at the OWC, and the smallest difference is at the GOC. However, the differences are difficult to detect with the addition of noise. More contrast between the original fluids and the substitute fluids and a less competent formation (smaller K_d) would increase the contrast between the synthetic gathers.

The P-S converted wave was modeled with the SYNTH AVO modeling program (Lawton and Howell, 1992). Figure 7 shows the original P-S gathers with 20% noise, the gas drive gathers with 20% noise, the difference gathers, the stacked gathers, and the stacked trace difference. Figure 8 is the same for the water drive case. The P-S converted wave reflection coefficient was calculated using velocity and density averaged 10 m above and below interfaces using Bortfeld's approximation (Bortfeld, 1961). Figure 9 shows the P-S reflections strengthening with offset until a maximum is reached followed by decreasing reflection strength. Fluid substitution has changed the incident angle of the maximum amplitude, although it is difficult to see on synthetic gathers (Figures 7 and 8). The differences are most pronounced at the GOC and

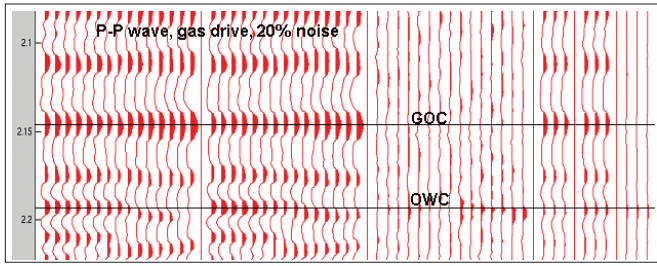


Figure 4. The original, gas drive P-P gather, their difference, stacked traces, and their difference.

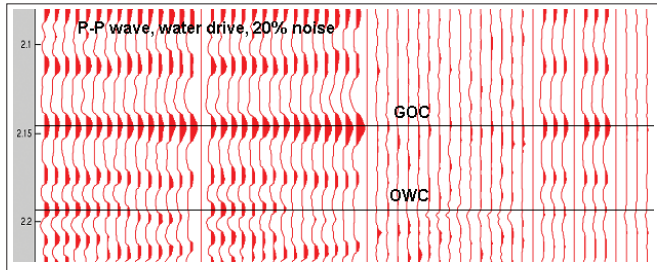


Figure 5. The original, water drive P-P gather, their difference, stacked traces, and their difference.

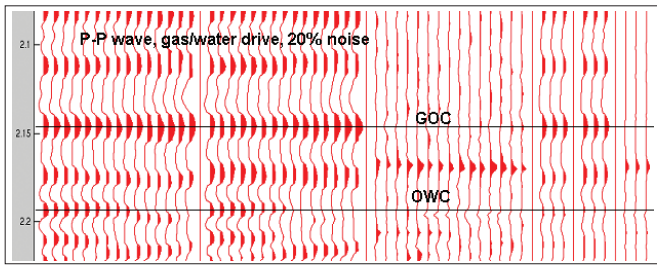


Figure 6. The original, gas/water drive P-P gather, their difference, stacked traces, and their difference.

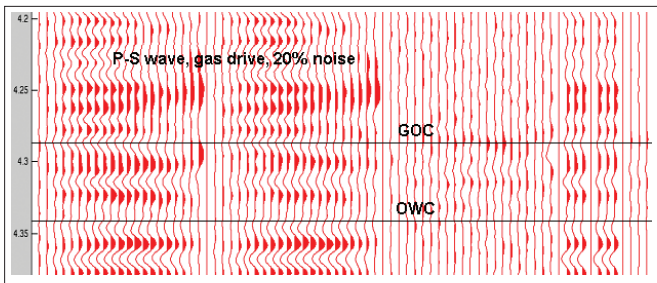


Figure 7. The original and gas drive P-S gather, their difference, stacked traces, and their difference.

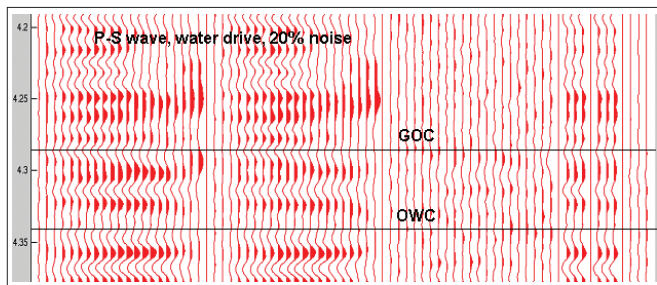


Figure 8. The original and water drive P-S gather, their difference, stacked traces, and their difference.

for the gas drive. Differences between the water drive and the original traces are not as strong as for the gas drive because V_s is sensitive to density changes, and the change in density due to water substitution for oil is less than the change in density due to gas substitution for oil. Interestingly, both the gas

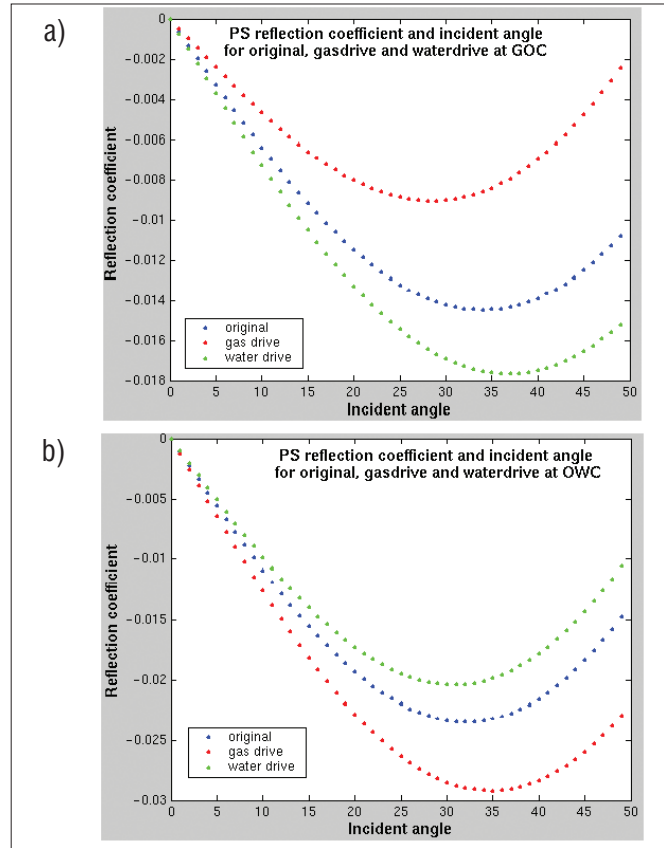


Figure 9. P-S reflection coefficient changes with incident angle for (a) at GOC and (b) at OWC.

and water drive P-S waves show a larger change for the cycle within the reservoir zone than the P-P synthetics.

The changes in the density and velocity are on the order of 1-2%, but visible, if subtle, changes can be seen on the synthetic seismograms. As an example, consider the GOC for the zero-offset P-P case. The reflection coefficient at zero-offset is R_o and $\Delta R_o/R_o = 2I_1\Delta I_2/(I_2^2 - I_1^2)$ is the percentage change in R_o due to a change in acoustic impedance I_2 . Averaging the original logs over the 10 m adjacent to the GOC, we find that $I_1 = 9321 \text{ m/s g/cm}^3$ and $I_2 = 10085 \text{ m/s g/cm}^3$. After gas substitution $\Delta I_2 = -137 \text{ m/s g/cm}^3$, $\Delta I_2/I_2 = 1.3\%$, and $\Delta R_o/R_o = -17\%$. Although impedance changes slightly more than 1%, the percentage change in the reflection coefficient is much greater.

Conclusions. Substitution of reservoir oil by gas and water can cause changes in seismic and AVO response that can be modeled using well logs and reservoir parameters. These modeling studies can be used as part of a feasibility study for specific reservoir monitoring objectives using time-lapse seismic surveys. The studies can also be useful for interpreting the results of time-lapse surveys.

Using a well log from White Rose Field, our modeling study predicts that gas or water drives will cause changes in the zero-offset reflection coefficients on the order of 15%. Greater contrast between the original fluid and the substitute fluid causes larger differences on the seismic traces. Due to the relatively high value of the dry bulk modulus, K_d , and the moderate porosity, the influence of the fluid saturation changes is relatively small. It appears that most of the change in seismic response is due to the density change during the fluid substitution. AIP changes for both gas drive and water drives are -1.5% and 1.6%, respectively. Changes are visible in the

(Continued on p. 566)

(Zou, from p. 554)

synthetic traces, but most are subtle. Since the acoustic impedance changes are less than 4%, differences may be difficult to detect on field data.

The substitution of different fluids causes 17% changes in the zero offset P-P reflection coefficient but only minor changes to the gradient of P-P AVO reflection coefficient curves. On the other hand, fluid substitution causes the maximum P-S amplitude offset position to change. Potentially, it may be used to distinguish zones where water or gas has displaced oil from unswept zones.

Suggested reading. "Seismic properties of pore fluids" by Batzle and Wang (GEOPHYSICS, 1992). "Evaluating feasibility of seismic fluid monitoring" by Bentley et al. (SEG Expanded Abstracts, 2000).

"Approximation to the reflection and transmission coefficients of plane longitudinal and transverse waves" by Bortfeld (*Geophysical Prospecting*, 1961). "P-P and P-SV synthetic stacks" by Lawton and Howell (SEG Expanded Abstracts, 1992). "Practical issues of 4D seismic reservoir monitoring: What an engineer needs to know" by Lumley and Behrens (*SPE Reservoir Evaluation & Engineering*, 1998). "Correlations for fluid physical property predictions" by Vasques and Beggs (*JPT*, 1980). [T|E](#)

Acknowledgments: We thank the CREWES sponsors for their support of this research. Special thanks to Husky Oil for providing the data used in this study and to Hampson-Russell for use of its software. We thank Jon Downton for reviewing our work and suggestions.

Corresponding author: zou@geo.ucalgary.ca